

Development 140, 2879–2891 (2013) doi:10.1242/dev.089326
 © 2013. Published by The Company of Biologists Ltd

Defining skeletal muscle resident progenitors and their cell fate potentials

Alice Pannérec*, Luigi Formicola*, Vanessa Besson, Giovanna Marazzi† and David A. Sassoon†

SUMMARY

The satellite cell is the major tissue-resident stem cell underlying muscle regeneration; however, multiple non-satellite myogenic progenitors as well as non-myogenic populations that support the muscle regenerative process have been identified. PW1 is expressed in satellite cells as well as in a subset of interstitial cells with myogenic potential termed PICs (PW1+ interstitial cells). Microarray profiling revealed that PICs express a broad range of genes common to mesenchymal stem cells, whereas satellite cells express genes consistent with a committed myogenic progenitor. Isolated PICs from both young and adult muscles can differentiate into smooth and skeletal muscle and fat whereas satellite cells are restricted to a skeletal muscle fate. We demonstrate that the adipogenic potential of PICs corresponds to a subpopulation that expresses platelet derived growth factor receptor alpha (PDGFR α) and overlaps with the recently described interstitial adipogenic progenitors. By contrast, PICs with myogenic potential do not express PDGFR α . Moreover, we observe a discrete and transient population of juvenile PICs based upon SCA1 expression that disappears by 3 weeks of postnatal development coincident with a switch in the cellular and genetic mechanisms underlying postnatal muscle growth.

KEY WORDS: Skeletal muscle, PW1, Stem cell, PDGFR α , Mouse

INTRODUCTION

Since their initial identification (Mauro, 1961), extensive work has demonstrated that satellite cells constitute the major source of postnatal skeletal muscle progenitors (Montarras et al., 2005; Relaix et al., 2005; Zammit et al., 2006). However, multiple non-satellite cell populations possessing myogenic capacity that are either freely circulating or resident in the muscle interstitium and vessels have been described (Benchaouir et al., 2007; Dellavalle et al., 2007; Gussoni et al., 1999; Liadaki et al., 2012; Mitchell et al., 2010; Pannérec et al., 2012; Sampaioles et al., 2006; Sampaioles et al., 2003). Although these progenitors adopt a skeletal myogenic fate following engraftment into damaged or diseased muscle, their direct contribution to postnatal muscle growth and regeneration is unknown or limited (Dellavalle et al., 2011).

Purified satellite cells display robust myogenic differentiation *in vitro* (Bischoff, 1975; Konigsberg, 1961), suggesting a strong cell fate commitment to the myogenic program; however, specific interactions between satellite cells and other muscle resident cell populations have been demonstrated to occur *in vivo*. Specifically, resident interstitial cells can regulate the balance between myogenesis, adipogenesis and fibrogenesis during regeneration (Joe et al., 2010; Murphy et al., 2011; Uezumi et al., 2010). Connective tissue fibroblasts, identified by TCF4 expression, proliferate in close proximity to satellite cells in response to injury (Murphy et al., 2011) and depletion of TCF4+ cells prior to muscle damage leads to poor regeneration and a reduced replacement of satellite cells due to premature differentiation (Murphy et al., 2011). Two adipogenic progenitor populations have been identified in the adult muscle interstitium. These two populations have been isolated either by

PDGFR α expression (Uezumi et al., 2010) or from a SCA1 (LY6A) positive (SCA1+) population (Joe et al., 2010). Although it remains unclear whether these cell populations overlap, both populations display a strong adipogenic potential *in vitro* and differentiate into fat when engrafted in a model of fatty infiltration, but not in healthy muscle, suggesting that the cellular environment controls their fate. Fibro/adipogenic progenitors (FAPs) are activated upon injury and promote myoblast differentiation through cell-cell signaling but do not display myogenic potential (Joe et al., 2010). In turn, adipogenesis of PDGFR α + cells is strongly inhibited by the presence of myotubes (Uezumi et al., 2010). These data suggest that muscle homeostasis and regeneration is dependent upon a balance between satellite cell-dependent myogenesis and PDGFR α + cell- and FAP- dependent adipogenesis.

We identified previously a non-satellite cell population in early postnatal (juvenile) skeletal muscle characterized by PW1 (PEG3 – Mouse Genome Informatics) expression and its location in the interstitium; these cells are referred to as PICs (PW1+ interstitial cells) (Mitchell et al., 2010). PICs display myogenic potential *in vitro* and participate in the generation of new myofibers, satellite cells and PICs following engraftment into damaged muscle (Mitchell et al., 2010). Whereas lineage-tracing studies demonstrated that PICs and satellite cells do not share a common PAX3- and PAX7-expressing progenitor during development, PICs express both PAX3 and PAX7 as they acquire a myogenic fate (Mitchell et al., 2010). Coupled with the observation that PICs spontaneously form skeletal and smooth muscle *in vitro*, we suggested that PICs represent a highly plastic muscle resident progenitor. In our initial description of PICs, we limited our analyses to juvenile postnatal muscle owing to the technical limitations of sorting a pure population of PW1-expressing cells with available markers. We have since generated a PW1-reporter transgenic mouse carrying a bacterial artificial chromosome (BAC) with the PW1 locus driving β -galactosidase (PW1^{nlacZ}) (Besson et al., 2011). Analyses of adult PW1^{nlacZ} mice revealed that both reporter and endogenous PW1 gene and protein are expressed in a wide range of adult stem cell niches, including gut, skin, CNS and early hematopoietic stem cells (Besson et al., 2011). This study also

Myology Group, UMR S 787 INSERM, University of Pierre and Marie Curie Paris VI, Paris, 75634, France.

*These authors contributed equally to this work

†Authors for correspondence (giovanna.em.marazzi@gmail.com; david.a.sassoon@gmail.com)

Accepted 10 May 2013

demonstrated the persistence of PW1 expression in adult skeletal muscle satellite and interstitial cells (PICs), although the cell fate potential of these adult interstitial cells remained unaddressed (Besson et al., 2011).

In this study, we confirm that PICs and satellite cells are distinct myogenic progenitors and that juvenile and adult PICs have multiple cell fate potentials *in vitro*. In addition, we demonstrate that adult PICs can be separated into two different populations with distinct cell fate potentials. The majority of adult PICs express PDGFR α and account for the two recently identified populations of fibro/adipogenic progenitors (Joe et al., 2010; Uezumi et al., 2010; Uezumi et al., 2011), but a small subset of PICs constitute an adult non-satellite cell population with myogenic potential. We find that the PICs that express intermediate levels of SCA1 are present only during the first 3 weeks of age, suggesting a role in postnatal muscle growth, whereas PICs that express high levels of SCA1 are present throughout postnatal and adult life. Results shown here indicate that PW1 expression defines all muscle resident stem/progenitor cells regardless of lineage.

MATERIALS AND METHODS

Mice

Animal models used were C57Bl6J *PW1^{IRESnLacZ}* transgenic reporter mice (*PW1^{nLacZ}*), in which a nuclear operon lactose gene is expressed under the control of the *Pw1* locus (Besson et al., 2011); and C57Bl6J mice (Elevage Janvier). All work with mice was carried out in adherence to French government and European guidelines.

Fluorescence-activated cell sorting analysis

For fluorescence-activated cell sorting (FACS), limb muscles from 1- to 7-week-old *PW1^{nLacZ}* or C57Bl6J mice were minced and digested in Hank's Balanced Salt Solution (HBSS; GIBCO) containing 2 $\mu\text{g ml}^{-1}$ collagenase A (Roche), 2.4 U ml^{-1} dispase I (Roche), 10 ng ml^{-1} DNase I (Roche), 0.4 mM CaCl_2 and 5 mM MgCl_2 as described previously (Besson et al., 2011; Mitchell et al., 2010). Primary antibodies at a concentration of 10 ng ml^{-1} were: rat anti-mouse CD45-APC (BD Biosciences), rat anti-mouse Ter119-APC (BD Biosciences), rat anti-mouse CD34-E450 (eBiosciences), rat anti-mouse Sca1-A700 (eBiosciences) and rat anti-mouse PDGFR α -PE (CD104a, eBiosciences). Cells were incubated for 30 minutes on ice. Cell pellets were washed twice before incubation with 5-dodecanoylamino fluorescein di- β -D-galactopyranoside (C_{12}FDG , 60 μM ; Life Technologies) for 1 hour at 37°C. Cells were washed once with ice-cold HBSS, filtered and re-suspended in HBSS containing 0.2% (w/v) bovine serum albumin (BSA), 1% (v/v) penicillin-streptomycin and 10 ng ml^{-1} DNase I. Flow cytometry analysis and cell sorting were performed on a FACSaria (Becton Dickinson) with appropriate isotype matching controls (supplementary material Fig. S1). TER119 (LY76)+ and CD45 (PTPRC, LY5)+ cells were negatively selected and the remaining cells were gated based on their CD34 and SCA1 expression. PDGFR α positive or negative cells were sorted in the SCA1^{HIGH}/PW1+ and SCA1^{HIGH}/PW1- fractions as well as the SCA1^{MED} fraction. Purified cell populations were cultured as described below. For immunocytochemical analyses, freshly sorted cells (4000 cells per well) were immediately centrifuged in 96-well plate (Becton Dickinson) coated with 0.1% porcine gelatin (Sigma) and subsequently reacted with X-Gal as described previously (Gross and Morgan, 1999). For immunofluorescence analyses, freshly sorted cells were immediately centrifuged onto 8-well chamber glass slides (10,000 cells per well) (Thermo Scientific) for 5 minutes at 100 g and immunostained for PW1 and PAX7 or PDGFR α , as described below. Quantitative analyses were performed by counting the number of positive cells out of a minimum of 300 cells in randomly chosen fields for each of three independent experiments.

Cell culture

Cells from limb muscles of 1- to 7-week-old mice were obtained as described above. Immediately after sorting, cells were plated on gelatin-coated dishes at a density of 2000 cells per cm^2 for myogenic differentiation and at a density of 6000 cells per cm^2 for adipogenic differentiation. Cells were grown for one

week in high-glucose Dulbecco's modified Eagle medium (DMEM; Gibco) supplemented with 2.5 ng ml^{-1} basic fibroblast growth factor (bFGF; Invitrogen), 20% heat-inactivated fetal bovine serum (FBS; Invitrogen), 10% heat-inactivated horse serum (Gibco), 1% (v/v) penicillin-streptomycin (Gibco), 1% (v/v) L-glutamine (Gibco) and 1% (v/v) sodium pyruvate (Gibco). This growth medium (GM) was changed every 2 days. For myogenic differentiation, cells were transferred to differentiation medium [DM; DMEM containing 5% (v/v) horse serum and 1% (v/v) penicillin-streptomycin] for 2 days. For adipogenic differentiation, cells were transferred to adipogenic differentiation medium [ADM; DMEM containing 20% (v/v) FBS, 1% (v/v) penicillin-streptomycin, 0.25 μM dexamethasone (Sigma), 0.5 mM isobutylmethylxanthine (Sigma), 1 $\mu\text{g ml}^{-1}$ insulin (Sigma) and 5 μM troglitazone (Sigma)] for 5 days. Medium was changed every 2 days.

Histological analyses

Cryosections (10 μm) prepared from 7-week-old mice tibialis anterior snap frozen in liquid nitrogen-cooled isopentane, cultured cells and cytospin preparations were fixed in 4% (w/v) paraformaldehyde and processed for immunostaining as described previously (Mitchell et al., 2010). Primary antibodies were: anti-PW1 (Relaix et al., 1996), anti-PAX7 (Developmental Studies Hybridoma Bank), anti-laminin (Sigma), anti-MyoD (BD Biosciences), alpha-smooth muscle actin (Sigma), anti-SM22-alpha (Abcam), anti-MF20 (Developmental Studies Hybridoma Bank), anti-Ki67 (BD Biosciences) and biotinylated anti-PDGFR α -biotin (2.5 ng ml^{-1} ; R&D Systems). Antibody binding was revealed using species-specific secondary antibodies coupled to Alexa Fluor 488 (Molecular Probes), Cy3 or Cy5 (Jackson ImmunoResearch). Nuclei were counterstained with DAPI (Sigma). To stain lipids, cells were fixed in 10% formalin (Sigma) for 5 minutes at 4°C, rinsed in water and then 100% propylene glycol (Sigma) for 10 minutes, stained with Oil Red O (Sigma) for 10 minutes at 60°C, placed in 85% propylene glycol for 2 minutes and rinsed in water. Nuclei were counterstained with Mayer's Hematoxylin Solution (Sigma). Cells in culture were quantified by counting at least 300 cells from randomly chosen fields for each of three independent experiments. Fusion indexes were quantified by counting the number of nuclei in MF20+ cells/total number of nuclei (Coletti et al., 2002; Mitchell et al., 2010; Schwarzkopf et al., 2006). Adipogenic potential was quantified by counting the number of nuclei in Oil Red O+ cells per total number of nuclei. Images were acquired using a Leica DM-IL inverted fluorescence and light microscope, Leica DM fluorescence and light microscope or Leica SPE confocal microscope.

Microarray analysis

For microarray analysis (GeneChip MOE 430 2.0, Affymetrix), RNA was extracted from freshly FACS sorted PICs and satellite cells from 1-week-old C57Bl6 limb muscles, using RNeasy Micro Kit (Qiagen) according to manufacturer's recommendations. Three independent samples for each experimental group were sent for analysis to PartnerChip (Génopole d'Evry, France).

Statistical analysis was performed using a fold change threshold of 1 and a *P*-value threshold of 0.01. Subsequent analyses were performed using the Gene Ontology database. The microarray analysis has been deposited in NCBI's Gene Expression Omnibus under accession number GSE40523.

RNA extraction and RT-PCR

RNA extracts were prepared from a minimum of 2×10^4 freshly sorted cells using RNeasy Micro Kit (Qiagen) according to manufacturer's instructions, and reverse transcribed using the SuperScript First-Strand Synthesis System (Life Technologies). Semi-quantitative PCR was performed using ReddyMix Master Mix (Thermo Scientific) under the following cycling conditions: 94°C for 5 minutes followed by 30 cycles of amplification (94°C for 30 seconds, 60°C for 30 seconds and 72°C for 1 minute) and a final incubation at 72°C for 10 minutes. Primers are listed in supplementary material Table S1.

Statistical analysis

All statistical analyses were performed using an unpaired Student's *t*-test in the StatView software. Values represent the mean \pm s.e.m. **P*<0.05, ***P*<0.01 and ****P*<0.001.

RESULTS

Juvenile PICs and satellite cells have distinct gene expression profiles

We performed transcriptome analyses (Affymetrix) using RNA from wild-type PICs and satellite cells freshly isolated from 1-week-old murine limb muscles corresponding to a stage of active postnatal muscle growth. At this stage, satellite cells have not entered a completely quiescent state (Pallafacchina et al., 2010); nonetheless, PICs and satellite cells are clearly distinguishable based upon their location (sublaminal versus interstitial) and by the expression of

PAX7 (satellite cells) and PW1 (satellite cells and PICs) (Mitchell et al., 2010). We observed distinct transcriptome signatures with 1345 and 1233 genes expressed specifically in PICs and satellite cells, respectively (Fig. 1A). Gene Ontology database analyses revealed that satellite cell-specific genes are related primarily to the skeletal muscle lineage [i.e. *c-Met* (*Met*), *desmin*]. As expected, we observed the expression of genes known to be expressed in satellite cells and/or proliferating myoblasts (i.e. *Pax7*, myogenic regulatory factor genes, *Cxcr4*, integrin- $\alpha 7$, *Fgfr4*) (Fukada et al., 2007; Pallafacchina et al., 2010) (Fig. 1B). By contrast, PICs express

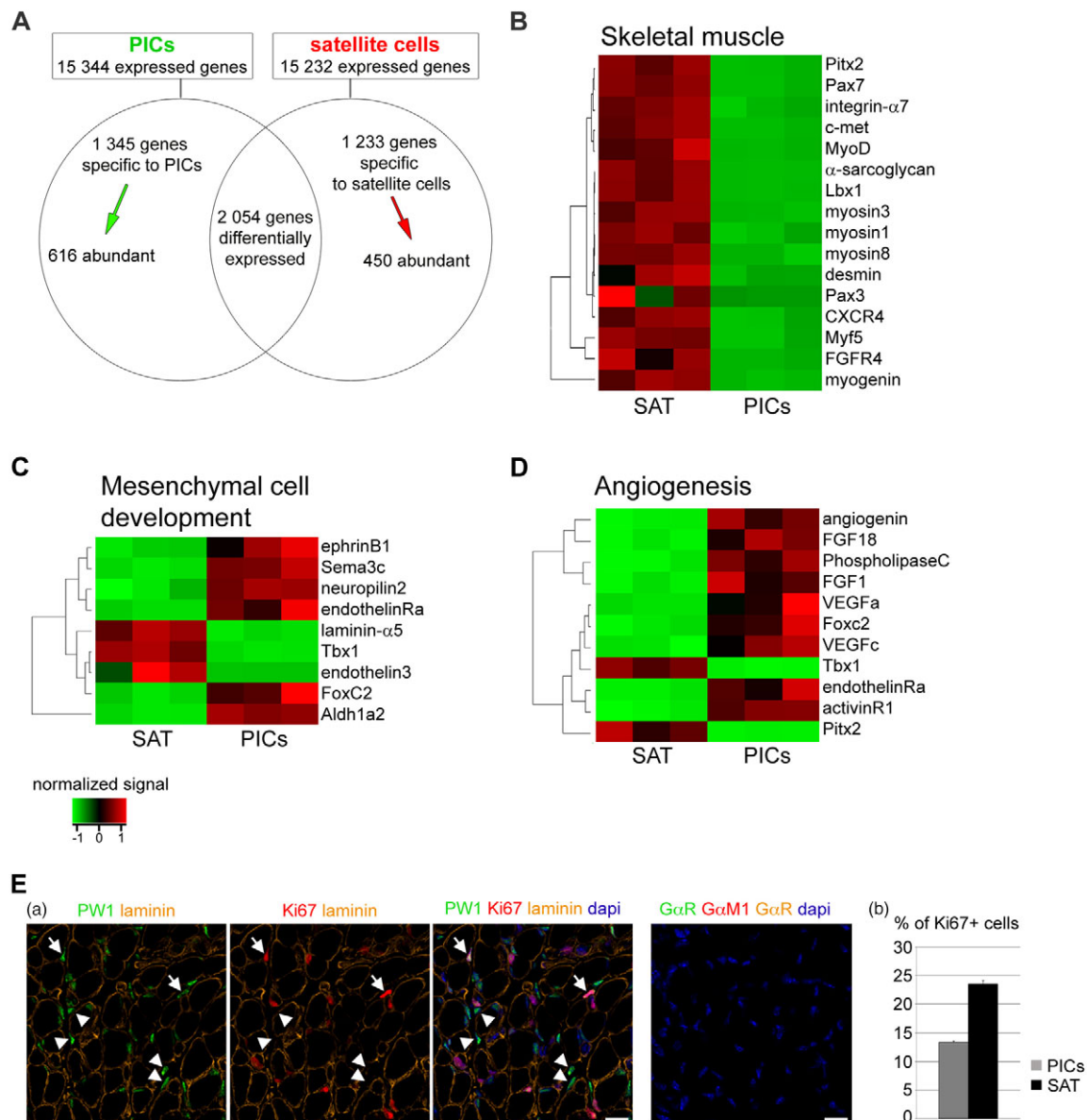


Fig. 1. PICs and satellite cells are distinct progenitors. (A) Venn diagram presenting the gene distribution of PICs and satellite cells. Data were obtained from Affymetrix microarray analysis of 1-week-old C57Bl6 mice with $n=3$ for each population. Fold change threshold=1, P -value threshold=0.01. (B–D) Gene Ontology clustering analysis for skeletal muscle (B), mesenchymal cell development (C) and angiogenesis (D) gene categories. The gene tree is shown on the left, and gene coloring was based on normalized signals as shown in the color bar. (E) (a) Cross-section of 1-week-old hindlimb muscle from C57Bl6 mice stained for PW1 (green) and the proliferation marker Ki67 (red). Laminin staining (orange) shows the basal lamina. Nuclei were counterstained by DAPI (blue). Arrows indicate proliferative PICs, arrowheads indicate quiescent PICs. Scale bars: 20 μ m. (b) Quantification of proliferative (Ki67+) PICs (gray) and satellite cells (black) for 1-week-old mice from cross-sections stained as shown in a. Values represent the mean number of positive satellite cells or PICs + s.e.m. per 100 cells. At least 500 cells for each cell type from three independent experiments were counted.

genes that are associated with multiple cell fates, including *Foxc2* and ephrins (mesenchymal stem cells), vascular endothelial growth factor and angiogenin (angiogenesis), and numerous genes governing cell interaction and cell migration (Fig. 1C,D). We confirmed the expression of PW1 in both cell types (<http://www.ncbi.nlm.nih.gov/geo/query/acc.cgi?acc=GSE40523>). We observed that specific growth factors and their cognate receptors were reciprocally expressed by PICs and satellite cells suggesting paracrine interactions between these two cell types (Tables 1, 2). We observed that *Pdgfra* was highly expressed in juvenile PICs compared with satellite cells (Table 1), suggesting that resident adipogenic populations (Joe et al., 2010; Uezumi et al., 2010) overlap with PICs. These analyses were performed using juvenile muscle in which the PICs and satellite cells are presumably not fully quiescent. We therefore verified the proliferative status of these populations by staining 1-week-old hindlimb muscle for the cell cycle marker Ki67. We observed that only ~15% of PICs and ~25% of satellite cells are cycling whereas the majority of these cell populations are quiescent (Fig. 1E). The distinct gene expression profiles observed here for juvenile satellite cells and PICs, combined with our previous analyses demonstrating that PICs do not arise from a PAX3 lineage (Mitchell et al., 2010), support the

hypothesis that PICs and satellite cells are distinct progenitor populations and that PICs represent a less committed progenitor compared with satellite cells. Furthermore, despite residual postnatal proliferative activity of satellite cells used for these analyses, we noted that the satellite cells have already assumed a gene expression profile closely resembling that found in adult satellite cells (Pallafacchina et al., 2010) (Fig. 3E).

Juvenile PICs display multiple potentials *in vitro*

We reported previously that PICs can be enriched from juvenile muscle (1-2 weeks of age) by sorting for the cell surface markers CD34 and SCA1 (Mitchell et al., 2010). At this stage, PICs are present in the CD34+/SCA1+ population, which can be subdivided into two populations based on SCA1 expression levels (SCA1^{MED} and SCA1^{HIGH}). In our previous study, we limited our analyses to the SCA1^{MED} population owing to the enriched number of PW1 cells in this fraction (>90%) (Mitchell et al., 2010). We were unable to isolate the PW1+ cells in the SCA1^{HIGH} population owing to a lack of appropriate markers. We have shown previously that the PW1^{nlacZ} reporter mouse allows for the purification of PW1-expressing cells using a fluorescent substrate (C₁₂FDG) for β -galactosidase activity from a wide array of tissues and that reporter

Table 1. Genes preferentially expressed by PICs

Gene symbol	Gene name	Average intensity*		Fold change [‡]	P-value
		PICs	SAT		
<i>Qprt</i>	quinolinate phosphoribosyltransferase	793	14	-62.7	0.0027
<i>P2ry14</i>	purinergic receptor P2Y, G-protein coupled, 14	1477	32	-46.5	0.0005
<i>Itgb3</i>	integrin beta 3	518	14	-41.4	0.0019
<i>Apod</i>	apolipoprotein D	1403	39	-39.1	0.0077
<i>Gpr133</i>	G protein-coupled receptor 133	438	13	-35.6	0.0025
<i>Aldh1a2</i>	aldehyde dehydrogenase family 1, subfamily A2	1444	49	-35.4	0.0048
<i>Myoc</i>	myocilin	1549	50	-35.2	0.0035
<i>Adam33</i>	a disintegrin and metallopeptidase domain 33	398	13	-34.8	0.0043
<i>Fst</i>	folliculin	381	11	-32.8	0.0073
<i>Foxd1</i>	forkhead box D1	724	21	-32.4	0.0025
<i>Ptch2</i>	patched homolog 2	840	35	-31.8	0.0094
<i>Il1rl2</i>	interleukin 1 receptor-like 2	499	19	-29.3	0.0027
<i>Pdgfra</i>	platelet derived growth factor receptor, alpha polypeptide	897	124	-28.3	0.0016
<i>Ebf2</i>	early B-cell factor 2	224	8	-28.1	0.0005
<i>Gjb2</i>	gap junction membrane channel protein beta 2	950	35	-27.3	0.0013
<i>Vtn</i>	vitronectin	1201	49	-26.2	0.0023
<i>Il15</i>	interleukin 15	204	8	-25.6	0.0005
<i>Cd55</i>	CD55 antigen	438	18	-25.2	0.0015
<i>Mmp16</i>	matrix metallopeptidase 16	892	44	-23.3	0.0066
<i>Arhgap20</i>	Rho GTPase activating protein 20	473	24	-22.8	0.0041
<i>Dnm1</i>	dynamitin 1	1517	91	-19.8	0.0084
<i>Avpr1a</i>	arginine vasopressin receptor 1A	331	20	-19.4	0.0088
<i>Adra2a</i>	adrenergic receptor, alpha 2a	369	21	-18.8	0.0040
<i>Bmp7</i>	bone morphogenetic protein 7	123	6	-18.2	0.0025
<i>Wnt5a</i>	wingless-related MMTV integration site 5A	1293	75	-18.1	0.0018
<i>Ednra</i>	endothelin receptor type A	261	15	-17.7	0.0026
<i>Ephb2</i>	ephrin receptor B2	300	19	-16.7	0.0030
<i>Pi15</i>	Peptidase inhibitor 15	171	12	-16.6	0.0083
<i>Fgf1</i>	fibroblast growth factor 1	462	31	-16.6	0.0060
<i>Twist1</i>	twist gene homolog 1 (Drosophila)	523	33	-16.5	0.0018
<i>Negr1</i>	neuronal growth regulator 1	136	8	-16.4	0.0012
<i>LepR</i>	leptin receptor	173	11	-16.2	0.0013
<i>Twist2</i>	twist homolog 2 (Drosophila)	114	7	-16.1	0.0013
<i>Efnb1</i>	ephrin B1	315	46	-6.7	0.0013
<i>Ng2</i>	chondroitin sulfate proteoglycan 4	965	153	-5.9	0.0107
<i>Pdgfrb</i>	platelet derived growth factor receptor, beta polypeptide	4916	1050	-4.8	0.0089
<i>Tgfb2</i>	transforming growth factor, beta receptor II	9019	2521	-3.6	0.0023

*For each gene, the average expression intensity was calculated from Affymetrix analysis.

[‡]SAT compared with PICs.

Table 2. Genes preferentially expressed by satellite cells

Gene symbol	Gene name	Average intensity*		Fold change [‡]	P-value
		PICs	SAT		
<i>Gpr50</i>	G-protein-coupled receptor 50	10	1012	117.6	0.0016
<i>Fgfr4</i>	fibroblast growth factor receptor 4	13	1032	86.5	0.0048
<i>Ryr1</i>	ryanodine receptor 1, skeletal muscle	8	640	80.8	0.0019
<i>Chrna1</i>	cholinergic receptor, nicotinic, alpha polypeptide 1 (muscle)	75	4851	74.8	0.0028
<i>Pitx3</i>	paired-like homeodomain transcription factor 3	4	310	68.9	0.0005
<i>Myod1</i>	myogenic differentiation 1	47	2275	57.1	0.0036
<i>Sgca</i>	sarcoglycan, alpha (dystrophin-associated glycoprotein)	6	350	55.6	0.0002
<i>Cdh15</i>	cadherin 15	59	2648	55.3	0.0040
<i>Lbx1</i>	ladybird homeobox homolog 1 (Drosophila)	7	332	48.4	0.0007
<i>Tnnt2</i>	troponin T2, cardiac	23	989	44.5	0.0014
<i>Pitx2</i>	paired-like homeodomain transcription factor 2	8	329	42.6	0.0007
<i>Traf3ip3</i>	TRAF3 interacting protein 3	21	891	41.6	0.0004
<i>Lama5</i>	laminin, alpha 5	13	364	33.8	0.0090
<i>Pde1c</i>	phosphodiesterase 1C	6	166	26.6	0.0005
<i>Arpp21</i>	cyclic AMP-regulated phosphoprotein, 21	13	349	26.1	0.0005
<i>Atp2a1</i>	ATPase, Ca++ transporting, cardiac muscle, fast twitch 1	64	1481	22.4	0.0022
<i>Tnik</i>	TRAF2 and NCK interacting kinase	28	593	22.0	0.0041
<i>Myh3</i>	myosin, heavy polypeptide 3, skeletal muscle, embryonic	18	378	21.3	0.0016
<i>Neb</i>	nebulin	7	155	21.1	0.0002
<i>Dcx</i>	doublecortin	10	194	19.5	0.0046
<i>Ephb1</i>	ephrin receptor B1	8	124	16.0	0.0016
<i>Chrn3</i>	cholinergic receptor, nicotinic, gamma polypeptide	8	134	15.8	0.0031
<i>Myh8</i>	myosin, heavy polypeptide 8, skeletal muscle, perinatal	21	289	15.5	0.0077
<i>Ank1</i>	ankyrin 1, erythroid	88	1245	15.4	0.0035
<i>Pdgfra</i>	platelet derived growth factor, alpha polypeptide	125	1532	13.7	0.0095
<i>Ppargc1b</i>	peroxisome proliferative activated receptor, gamma, coactivator 1 beta	12	154	13.3	0.0025
<i>Edn3</i>	endothelin 3	7	109	13.0	0.0089
<i>Tbx1</i>	T-box 1	9	109	11.7	0.0008
<i>Hdac11</i>	histone deacetylase 11	53	520	9.8	0.0009
<i>Des</i>	desmin	52	442	8.6	0.0091
<i>Gdf15</i>	growth differentiation factor 15	45	390	8.6	0.0074
<i>Drp2</i>	Dystrophin related protein 2	73	563	8.3	0.0066
<i>Tpm2</i>	tropomyosin 2, beta	17	134	8.1	0.0019
<i>Acvr2b</i>	activin receptor IIB	21	159	8.2	0.0148

*For each gene, the average expression intensity was calculated from Affymetrix analysis.

[‡]SAT compared with PICs.

expression corresponds to endogenous PW1 expression with >98% fidelity in these tissues, including skeletal muscle (Besson et al., 2011). We therefore used the PW1^{nLacZ} reporter mouse to purify PW1-expressing cells from juvenile muscle and observed reporter gene expression in satellite cells and in the SCA1_{MED} and SCA1_{HIGH} populations, as expected (Fig. 2A) (see Besson et al., 2011; Mitchell et al., 2010). SCA1_{MED} cells isolated from 1-week-old muscle were >90% pure for PW1 expression whereas the SCA1_{HIGH} fraction contained only 60% of PW1+ cells (Fig. 2A) (Mitchell et al., 2010), confirming that reporter expression in skeletal muscle reflected faithfully endogenous PW1 expression. We therefore used the PW1^{nLacZ} reporter mouse to sort the PW1+/SCA1_{HIGH} population to >90% purity (SCA1_{HIGH} PICs) (Fig. 2B). We compared and verified expression of a subset of genes from our microarray analysis in satellite cells, SCA1_{MED} PICs, SCA1_{HIGH} PICs and SCA1_{HIGH}/PW1- cells from 1-week-old hindlimb muscle (Fig. 2C). Neither population expressed the hematopoietic marker *Cd68*, demonstrating the reliability of the FACS sorting (Fig. 2C). As expected, only the satellite cell fraction expressed *Pax7*, *Myf5* and *Fgfr4* (Pallafacchina et al., 2010) consistent with our previous observations (Mitchell et al., 2010) and further demonstrating that the PIC fractions were not contaminated by satellite cells. We note that only PICs express *P2y14* (*P2ry14* – Mouse Genome Informatics) and *Qprt*, two of the most represented markers specific to PICs in our microarray analysis (Table 1). Interestingly, although

all populations expressed the embryonic marker vimentin, only the SCA1_{HIGH} PICs fraction expressed the mesenchymal marker *Tie2* (*Tek* – Mouse Genome Informatics), which has been shown recently to mark adipogenic progenitors, suggesting a link between these populations (Uezumi et al., 2010). This correlation was further confirmed by the fact that *Pdgfra* is highly expressed in both PIC fractions (Fig. 2C; Table 1). We showed previously that SCA1_{MED} PICs from juvenile mouse muscle are capable of differentiating into smooth and skeletal muscle *in vitro* (Mitchell et al., 2010). In order to test all PW1+ populations (satellite cells, SCA1_{MED} and SCA1_{HIGH} PICs), we purified these fractions using 1-week-old PW1^{nLacZ} reporter mice and tested their myogenic and adipogenic potentials (Fig. 2D,E). As expected, we observed that satellite cells are highly myogenic (fusion index >80%) and do not display detectable adipogenic capacity, whereas SCA1_{MED} PICs gave rise to skeletal muscle (fusion index=40%) and smooth muscle cells. In addition, the SCA1_{MED} PICs gave rise to adipocytes (adipogenic potential=40%) when cultured in adipogenic media (Fig. 2D,E). By contrast, SCA1_{HIGH} PICs displayed lower skeletal myogenic (fusion index=20%) and adipogenic potentials (30%) compared with SCA1_{MED} PICs (Fig. 2D,E). We noted that all PIC fractions displayed smooth muscle cell fates (Fig. 2D). In contrast to PICs, we found that SCA1_{HIGH}/PW1- cells adopt a smooth muscle phenotype but do not display myogenic or adipogenic potential (Fig. 2D,E).

The SCA1^{MED} PICs population is restricted to early postnatal stages

Having confirmed the reliability of the PW1^{nLacZ} reporter mouse and our FACS protocol in juvenile skeletal muscle, we set out to systematically isolate and test the lineage potential of PW1+ cells from both SCA1-expressing fractions throughout postnatal development and early adulthood. These analyses revealed a progressive decline of the SCA1^{MED} fraction during the first 3

weeks of life such that it was no longer detectable 5 weeks after birth (supplementary material Fig. S2). During this period, we observed that the SCA1^{HIGH} cell fraction increased from ~30% to ~70% of the CD45⁺/TER119⁺ muscle cells (supplementary material Fig. S2). Although the SCA1^{HIGH} cells increased in number, the proportion of PW1+ cells declined from ~60% to ~40% (supplementary material Fig. S2). We isolated PW1+ cells in the SCA1^{HIGH} fraction from 7-week-old PW1^{nLacZ} reporter mouse

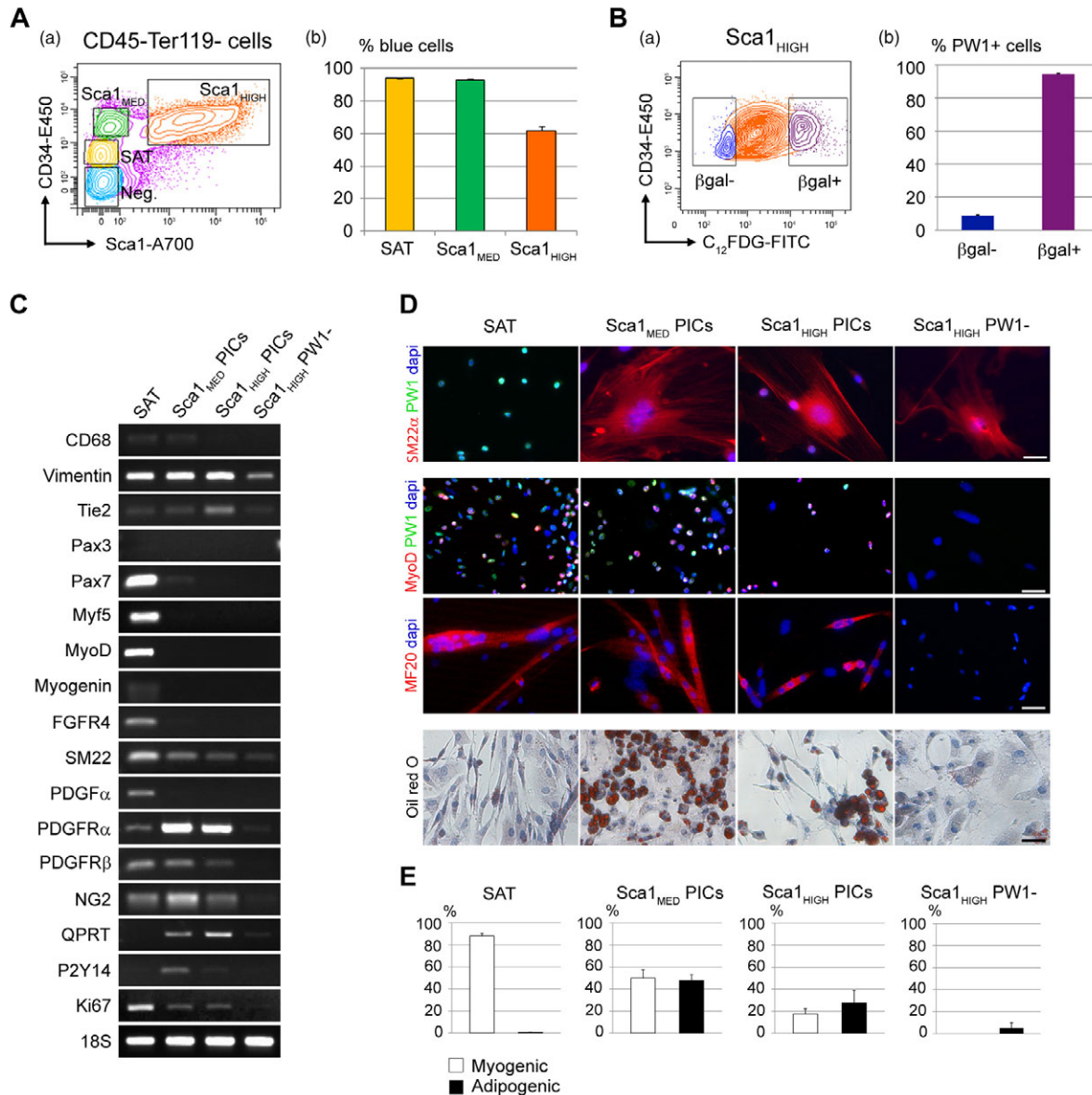


Fig. 2. Juvenile PICs display multiple potentials *in vitro*. (A) Flow cytometric analyses of single cells from 1-week-old PW1^{nLacZ} mice limb muscles stained with antibodies against SCA1 and CD34. CD45 and TER119^{HIGH} cells were excluded as described previously (Mitchell et al., 2010). The gates used to isolate CD34⁺/SCA1⁻, CD34⁺/SCA1^{MED} and CD34⁺/SCA1^{HIGH} cells are shown in a. The four fractions are indicated directly on the scatter plot (a). Reporter expression for each population was confirmed by β -galactosidase staining on freshly sorted cytopun cells and the percentage of β -galactosidase positive (β -gal⁺) cells was counted (b). (B) The CD34⁺/SCA1^{HIGH} population was sorted based on β -galactosidase expression (a). PW1 expression was confirmed by immunofluorescence on freshly sorted β -gal⁺ and β -gal⁻ cells and the percentages of PW1-expressing cells were counted. The CD34⁺/SCA1^{HIGH}/ β -gal⁺ fraction was ~94% positive for PW1 (b). (C) Semi-quantitative PCR of selected genes from our microarray analysis in satellite cells (SAT), SCA1^{MED} PICs, SCA1^{HIGH} PICs and SCA1^{HIGH}/PW1- cells freshly sorted as described above. (D) Representative images of FACS isolated populations grown in myogenic or adipogenic conditions and immunostained for the smooth muscle marker, SM22 α (top panel), myogenic markers (MyoD, MF20, middle panels) or stained with Oil Red O for adipocytic differentiation (bottom panel). Scale bars: 20 μ m. (E) Quantitative analysis of myogenic and adipogenic potential of cells treated as described in D. Myogenic values show the mean percentage + s.e.m. of nuclei incorporated into myotubes (MHC+ cells). Adipogenic values show the percentage of Oil Red O-positive cells. For all graphs, values are presented as percentage of positive cells + s.e.m. from at least three independent experiments.

muscle using C₁₂FDG as described for the juvenile muscle (Fig. 2B; Fig. 3A). We verified reporter and PW1 expression in freshly sorted cytopun cells as previously described (Besson et al., 2011) (Fig. 3B). We verified PAX7 expression to confirm the purity of the

satellite and non-satellite cell fractions (Fig. 3B). These data revealed that the SCA1_{MED} population of PICs is restricted to the first 3 weeks of postnatal life, raising the question of what stem cell potential, if any, is present in the SCA1_{HIGH} population.

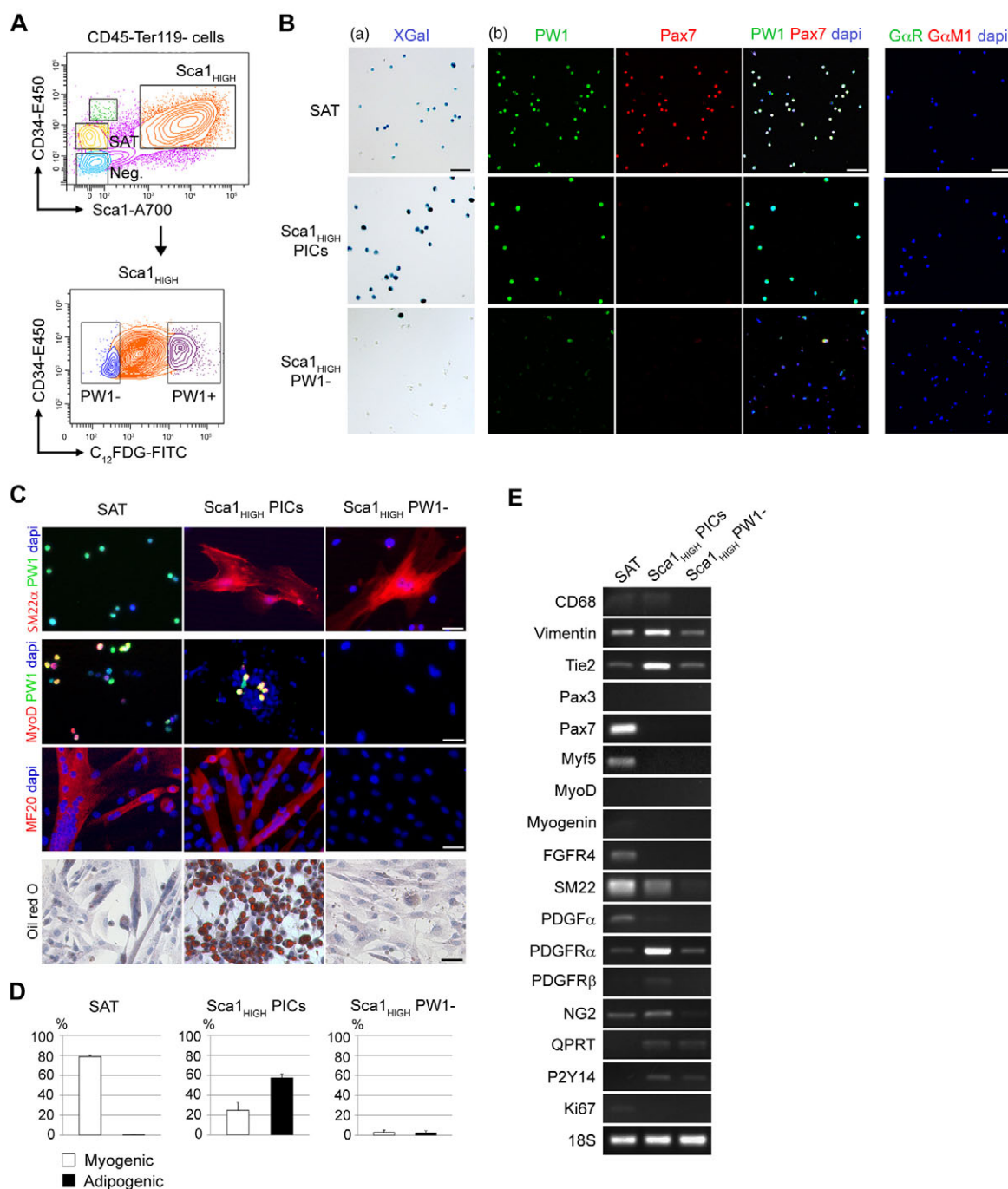


Fig. 3. Adult PICs show multiple lineage capacities. (A) Flow cytometric analyses of single cells from 7-week-old PW1^{nLacZ} mice limb muscles stained for CD45, TER119, CD34, SCA1 and C₁₂FDG. The gates used to isolate CD34+/SCA1⁻ (SAT), CD34+/SCA1^{HIGH}/PW1⁺ (PW1⁺) and CD34+/SCA1^{HIGH}/PW1⁻ (PW1⁻) populations are shown. (B) Histochemical (a) and immunolocalization (b) of PW1 (green) and PAX7 (red) in freshly sorted cytopun cell fractions, as shown in a. Nuclei are shown by DAPI staining (blue). Secondary antibody controls (primary antibody omitted) are shown (b, right column). Scale bars: 30 μm. (C) Representative images of FACS-isolated populations grown in myogenic or adipogenic conditions and immunostained for the smooth muscle marker (SM22α, top panel) and myogenic markers (MyoD, MF20, middle panels) or histochemically stained for adipocytic differentiation (Oil Red O, bottom panel). Nuclei were counterstained by DAPI (blue) or hematoxylin. Scale bars: 20 μm. (D) Quantitative analysis of myogenic and adipogenic potential of cells treated as described in C. Myogenic values show the mean percentage + s.e.m. of nuclei incorporated into MHC+ cells. Adipogenic values show the percentage of Oil Red O-positive cells. (E) Semi-quantitative PCR of selected genes from the microarray analysis in freshly sorted cell fractions, as shown in A.

Adult PICs display multiple cell fates *in vitro*

We next tested the myogenic (skeletal and smooth) and adipogenic potential of all PW1+ populations (satellite cells, SCA1^{HIGH} PICs) in adult muscle (7 weeks) (Fig. 3C). As expected, adult satellite cells were highly myogenic (fusion index=80%) and did not form smooth muscle or fat. Adult PICs generated skeletal muscle (fusion index=25%), smooth muscle and fat (adipogenic potential=60%) (Fig. 3C,D). By contrast, the SCA1^{HIGH}/PW1– cells did not show any myogenic or adipogenic potential but adopted a smooth muscle-like phenotype. Semi-quantitative PCR analysis showed no expression of *Pax7* and myogenic markers in the adult SCA1^{HIGH} PICs, confirming the reliability of our purification protocol. We note that adult SCA1^{HIGH} and juvenile SCA1^{HIGH} PICs show a similar gene profile (Fig. 3E). Notably, both juvenile and adult SCA1^{HIGH} PICs express *Tie2* and *Pdgfra*, consistent with an adipogenic potential (Uezumi et al., 2010; Uezumi et al., 2011) (Fig. 2C; Fig. 3E). We next examined whether cell fate potentials of PICs changed during the juvenile-to-adult transition. We found that the PW1– cells do not display myogenic or adipogenic capacity at any of the stages examined (supplementary material Figs S3–S5). Up to 3 weeks of postnatal development, when the SCA1^{MED} PIC population is still detectable, we found that this fraction retains the capacity to form fat and skeletal muscle (supplementary material Figs S3, S4). Although the SCA1^{HIGH} PIC population also shows a similar cell fate potential, we noted that this fraction was more adipogenic (supplementary material Figs S3, S4). At 5 weeks, when we no longer detect the SCA1^{MED} PICs, we observed a much higher skeletal myogenic capacity (~20%) in the SCA1^{HIGH} PIC population (supplementary material Fig. S4) similar to what we observed at 7 weeks of age. Taken together, these results demonstrate that PW1 identifies multiple progenitor populations in adult and juvenile skeletal muscle.

Adipogenic progenitors constitute a subpopulation of PICs

Adult skeletal muscle contains resident progenitor cells that can adopt an adipogenic fate under pathological conditions (Joe et al., 2010; Uezumi et al., 2010). These adipogenic progenitors had been isolated previously based upon SCA1 expression (Joe et al., 2010) or co-expression of SCA1 and PDGFR α (Uezumi et al., 2010). The potential overlap of these interstitial adipogenic progenitors (referred to here as IAPs) had not been elucidated; however, the population of SCA1+/PDGFR α + cells is presumably contained within the SCA1+ population. We observed that both juvenile and adult PICs expressed high levels of PDGFR α and display significant adipogenic potential (Figs 1–3). We therefore determined whether PICs and IAPs represent distinct or overlapping populations in the adult. Histological analyses of 7-week-old mouse tibialis anterior revealed that PW1 was co-expressed with PDGFR α in interstitial cells, but not all PW1+ cells express PDGFR α (Fig. 4A). As reported by Uezumi and colleagues (Uezumi et al., 2010), and confirmed in our studies here (Fig. 2C; Fig. 3E), PDGFR α expression is restricted to the SCA1+ cells in muscle. We therefore isolated PDGFR α -positive and -negative cells from the total SCA1^{HIGH} fraction to assess PW1 expression (Fig. 4B). Immunostaining for PW1 and PDGFR α on freshly isolated cells revealed that all PDGFR α + cells in the SCA1^{HIGH} fraction expressed PW1 whereas the PDGFR α -negative cells from the SCA1^{HIGH} fraction contained a small proportion of cells expressing PW1 (12 \pm 0.9%) (Fig. 4E). We next tested the SCA1^{HIGH}/PDGFR α + and SCA1^{HIGH}/PDGFR α – populations for myogenic and adipogenic potential and observed that adipogenic potential was restricted to

the SCA1^{HIGH}/PDGFR α + population (Fig. 4C,D) consistent with previously reported results (Uezumi et al., 2010). The SCA1^{HIGH}/PDGFR α – population did not display any myogenic or adipogenic potential. We next separated the SCA1^{HIGH} population on the basis of PW1 reporter gene expression and PDGFR α to obtain PDGFR α + and PDGFR α – PICs (Fig. 5A). As expected, the PDGFR α + PICs did not form any myogenic colonies but were strongly adipogenic (adipogenic potential=60%) (Fig. 5B,C). These differentiated adipocytes expressed genes related to adipogenesis (e.g. *Fabp4*; also known as *Ap2*) as well as genes specific to brown adipose tissue specific markers (*Ucp1*, *Prdm16*) and white/‘beige’ fat (*Hoxc9*) (Fig. 5F). By contrast, the PDGFR α – PICs were highly myogenic (fusion index=50%) but did not display adipogenic capacity (Fig. 5B,C). Fraction purity was confirmed by immunofluorescence for PAX7 and PW1 on freshly sorted cytopun cells (Fig. 5D) as well as by semi-quantitative PCR on freshly sorted cells (Fig. 5E). All PIC populations were negative for *Pax7* and myogenic genes. Only the PDGFR α + PICs express the adipogenic markers *Tie2* and *Pdgfra*, as expected. Taken together, these results demonstrate that adult PICs can be separated by PDGFR α expression into two distinct populations with different cell fate potentials.

We have shown that adult PICs and juvenile SCA1^{MED} and SCA1^{HIGH} PICs express *Pdgfra*, whereas only adult and juvenile SCA1^{HIGH} PICs express *Tie2* (Fig. 2C; Fig. 3E). We therefore separated juvenile (1 week old) SCA1^{MED} and SCA1^{HIGH} PICs based on PDGFR α expression and tested their myogenic and adipogenic potentials. As expected, only the PDGFR α – fractions (SCA1^{MED} and SCA1^{HIGH}) displayed myogenic capacity. Surprisingly, the juvenile SCA1^{MED}/PDGFR α + cells were weakly adipogenic (~5%) (Fig. 6) compared with the total SCA1^{MED} fraction (~35% adipogenic potential; Fig. 2D,E), suggesting that cell-cell interactions regulate cell fate outcomes. Juvenile SCA1^{HIGH}/PDGFR α + PICs, like adult SCA1^{HIGH}/PDGFR α + PICs, were strongly adipogenic (~40% adipogenic potential) (Fig. 6).

DISCUSSION

We described previously a non-satellite cell progenitor population in the interstitium of postnatal muscle referred to as PICs (Mitchell et al., 2010). Although satellite cells and PICs express PW1, satellite cells are strongly committed to the skeletal muscle lineage whereas a single PIC can generate both smooth and skeletal muscle *in vitro* (Mitchell et al., 2010). Genetic lineage-tracing studies demonstrated that PICs and satellite cells do not share a common progenitor (e.g. PAX3-derived) despite their shared skeletal muscle potential (Mitchell et al., 2010). The different lineage origins of PICs and satellite cells are further underscored by results obtained here in which we show that PICs and satellite cells have distinct transcriptome signatures in both juvenile and adult stages. Even though our Affymetric-based screen used juvenile (10-day-old) satellite cells, we found that genes that have been ascribed to adult, and therefore fully quiescent satellite cells, are expressed, including *Pax7*, *Fgfr4* and *c-Met*, whereas we noted the expression of *Myf5* and *Ki67* consistent with a more activated state (Figs 1, 2). During postnatal growth, we observed that PICs express many genes that play key roles during angiogenesis, including the pericyte marker *Ng2* (Dellavalle et al., 2007). Pericytes are vessel-associated cells that have also been shown to possess myogenic potential and are proposed to be the muscle-resident postnatal equivalent of mesoangioblasts (Dellavalle et al., 2007; Sampaolesi et al., 2003). Similar to PICs, mesoangioblasts contribute to new myofibers following engraftment into damaged muscle (Sampaolesi et al.,

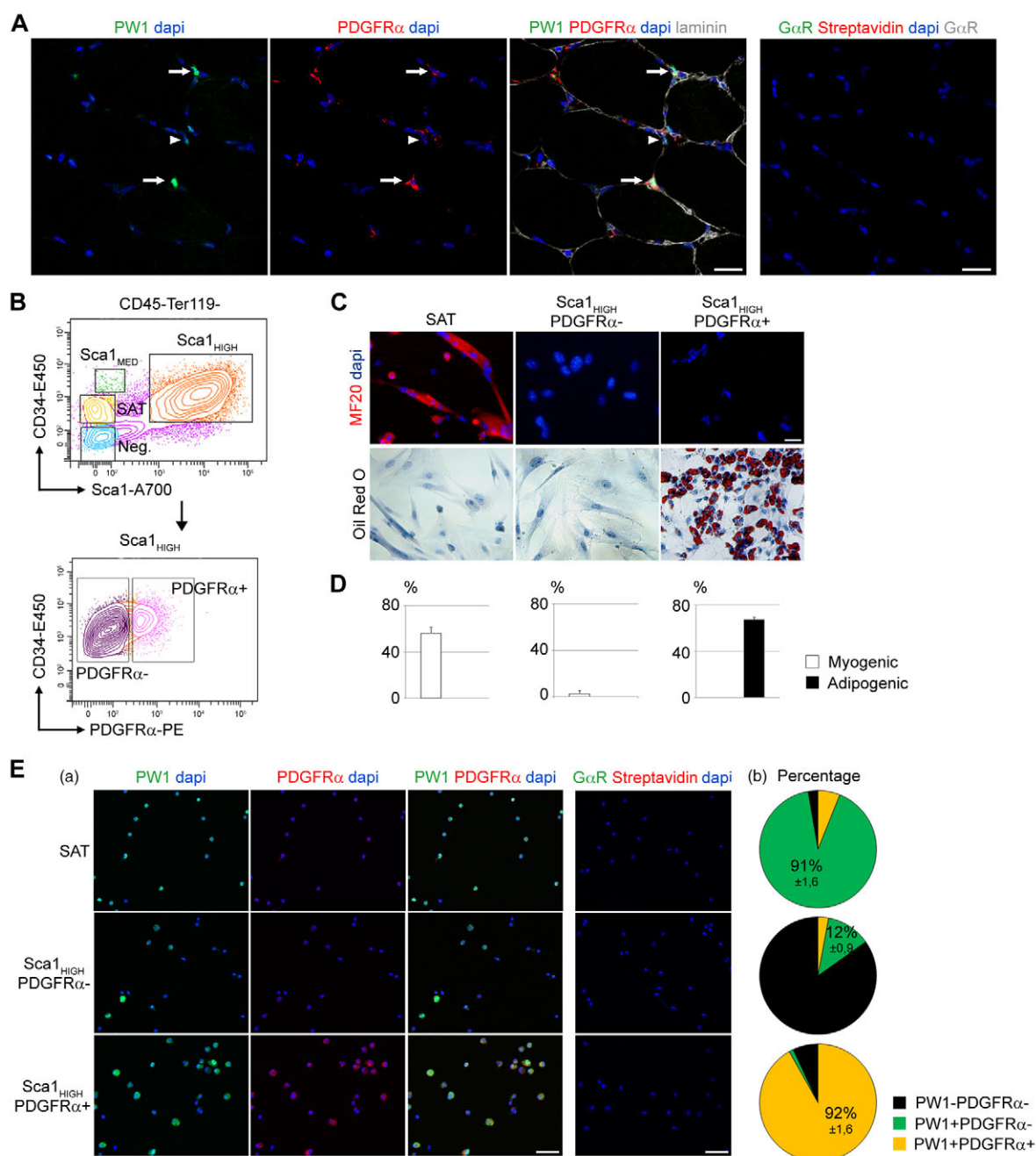


Fig. 4. IAPs constitute a subpopulation of PICs. (A) Cross-section of a 7-week-old tibialis anterior muscle immunostained for PW1 (green), PDGFRα (red) and laminin (gray). Nuclei were counterstained by DAPI (blue). Species-specific antibodies controls are shown. Arrows indicate PDGFRα+ cells, arrowheads indicate PICs, which do not express PDGFRα. (B) FACS isolation of PDGFRα+ and PDGFRα- cells from 7-week-old SCA1^{HIGH} cells. (C) Representative images of FACS-sorted populations cultured under myogenic or adipogenic conditions, immunostained for the myogenic marker (MF20, top panels) or histochemically stained for adipocytic differentiation (Oil Red O, bottom panel). (D) Quantification of myogenic and adipogenic potentials of cells treated as described in C. Values represent the mean + s.e.m., *n*=3 independent experiments for each condition. (E) (a) Immunolocalization of PW1 (green) and PDGFRα (red) in freshly sorted cytospun cell fractions, as shown in B. Nuclei were counterstained by DAPI (blue). Secondary antibody controls (primary antibody omitted) are shown. (b) Quantification of cells positive or negative for PW1 and PDGFRα. Values show the mean percentage ± s.e.m. of positive cells from three independent experiments. Scale bars: 20 μm.

2006; Sampaolesi et al., 2003) and show a mesenchymal and vascular-like profile (Brunelli et al., 2004). We note that mesoangioblasts express high levels of PW1 as well as PDGFRα (Pessina et al., 2012) suggesting a close relationship between these two skeletal muscle-resident stem cells. Whereas embryonic

mesoangioblasts derived from embryonic day 10.5 dorsal aorta express PAX3 and require PAX3 for myogenic and adipogenic differentiation (Messina et al., 2009), we note that PICs are not derived from a PAX3-expressing progenitor; however they do initiate PAX3 and PAX7 expression upon myogenic differentiation

(Mitchell et al., 2010). The precise relationship between PICs and mesoangioblasts remains to be fully elucidated.

In addition to non-satellite cell progenitors with myogenic potential, two recent reports have identified interstitially located cells with adipogenic potential (Joe et al., 2010; Schulz et al., 2011;

Uezumi et al., 2010). These cells, referred to as fibro/adipogenic progenitors (FAPs), and mesenchymal adipogenic progenitors were identified on the basis of high SCA1 expression and PDGFR α expression, respectively (Joe et al., 2010; Uezumi et al., 2010). It has been subsequently proposed that these two populations might be

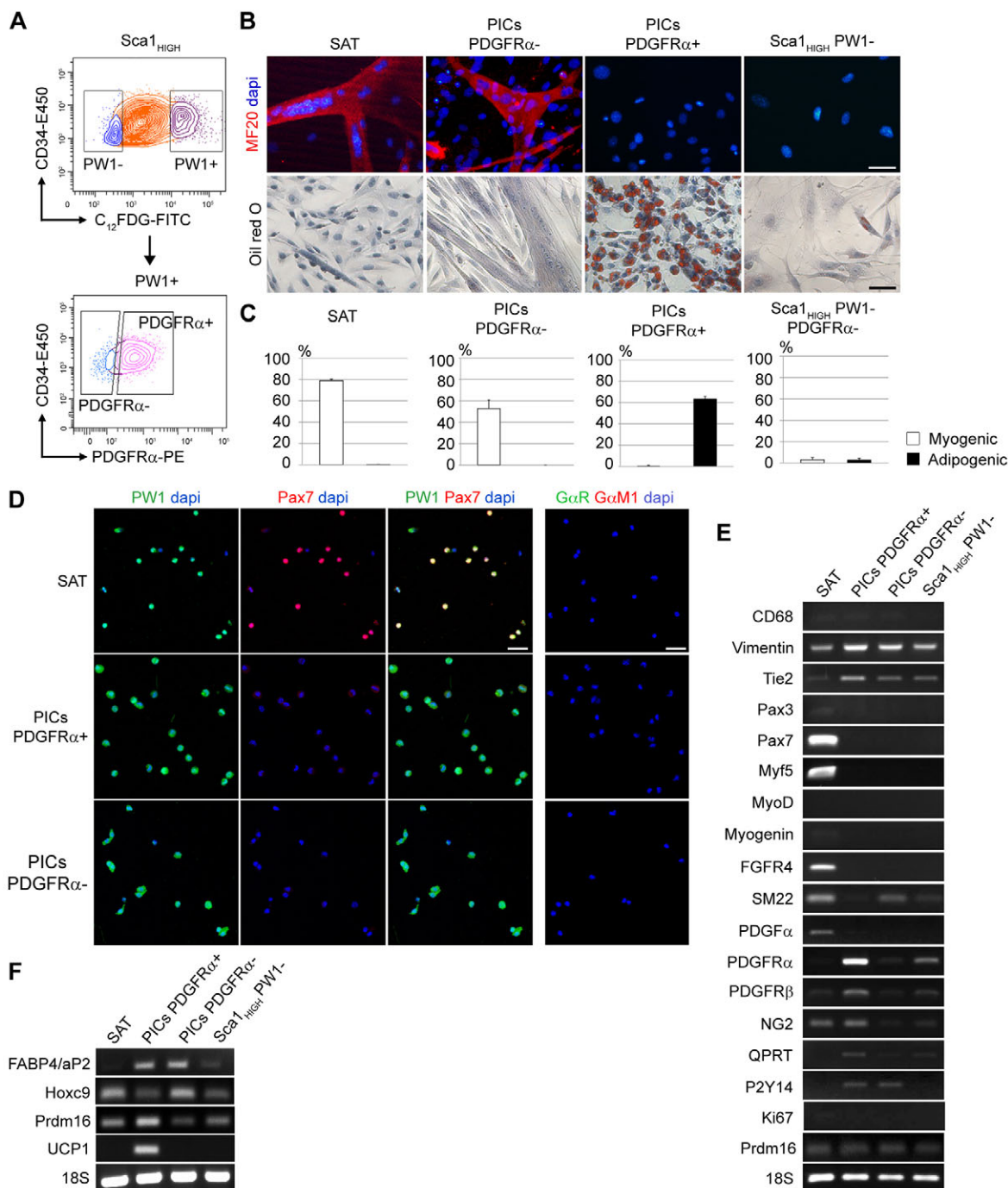


Fig. 5. Adult PICs cell fate can be identified by PDGFR α expression. (A) FACS isolation of PDGFR α ⁺ and PDGFR α ⁻ cells from 7-week-old SCA1^{HIGH}/PW1⁺ fraction. (B) Representative images of FACS-sorted populations cultured under myogenic (top panel) or adipogenic (bottom panel) conditions, immunostained for the myogenic marker (MF20, top panels) or histochemically stained for adipocytic differentiation (Oil Red O, bottom panel). Nuclei were counterstained by DAPI (blue) or hematoxylin. (C) Quantification of myogenic and adipogenic potentials of cells treated as described in B. Values are presented as percentage of positive cells + s.e.m. from at least three independent experiments for each condition. (D) Immunolocalization of PW1 (green) and PAX7 (red) in freshly sorted cytospun cell fractions, as shown in A. Nuclei are shown by DAPI staining (blue). Secondary antibody controls (primary antibody omitted) are shown. (E) Semi-quantitative PCR of selected genes from microarray analysis in freshly sorted cell fractions, as shown in A. (F) Semi-quantitative PCR of adipocyte specific genes in FACS-sorted populations cultured under adipogenic conditions. Scale bars: 20 μ m.

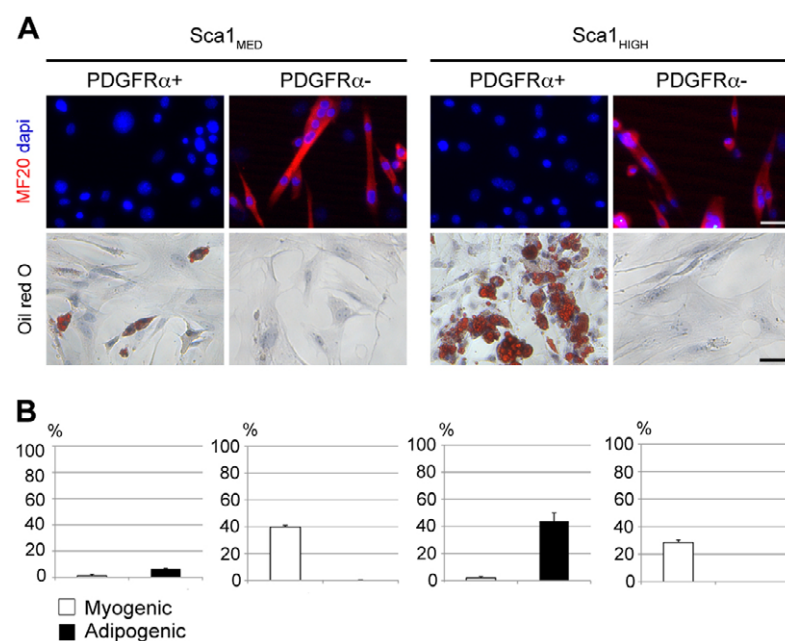


Fig. 6. PDGFR α expression is absent in myogenic juvenile PICs. (A) Isolated juvenile PIC populations separated on the basis of PDGFR α expression grown in myogenic (top panel) or adipogenic (bottom panel) conditions. Scale bars: 20 μ m. (B) Quantification of myogenic and adipogenic potentials of cells presented in A. Values are presented as percentage of positive cells + s.e.m. from at least three independent experiments.

partially or completely overlapping (Natarajan et al., 2010). Although these cells do not contribute directly to the generation of new myofibers in response to injury, they exert a pro-myogenic effect on satellite cells *in vitro* through paracrine signaling (Joe et al., 2010). More recently, a study has described that white adipose tissue present in skeletal muscle contains a population of highly inducible brown fat ('beige') progenitors that express SCA1 and PDGFR α (Schulz et al., 2011). These interstitial adipogenic populations (referred to here collectively as IAPs) are also proposed to be the source of ectopic fat deposition in diseased muscle owing to their ability to form fat *in vitro* and upon grafting either into diseased muscle or into pro-adipogenic sites *in vivo* (Joe et al., 2010; Uezumi et al., 2010). Because IAPs and PICs express high levels of SCA1 and PDGFR α in the adult, we wondered whether PICs and IAPs constituted a partially overlapping population of progenitors. This hypothesis seemed likely given our recently reported observation that PW1 expression is found in all adult stem/progenitor cells examined to date, including blood, brain, bone, skin and gut (Besson et al., 2011). Thus, if PW1 serves as a pan-stem cell marker in adult tissues, we would expect PW1

expression to identify all progenitor cell types in a specific tissue containing a mixture of cell lineages, such as skeletal muscle. In this study, we used the PW1^{nlacZ} reporter mouse line (Besson et al., 2011) to purify PW1-expressing cells from skeletal muscle during postnatal development and in the adult in order to determine their cell fate potentials and specifically address the relationship of the various resident progenitor cells described to date. Our results demonstrate that IAPs constitute a sub-population of PICs that can be separated based upon PDGFR α expression. Specifically, PDGFR α ⁺ PICs are adipogenic progenitors whereas PDGFR α ⁻ PICs display myogenic potential. SCA1⁺/CD34⁺/PDGFR α ⁺ adipogenic progenitors have been recently shown to be present in abdominal murine white adipose tissue and are able to differentiate into both brown and white fat (Lee et al., 2012). Adipocyte progenitor cells isolated from skeletal muscle are highly committed to become brown fat, but can also give rise to white or 'beige' fat *in vitro* (Cannon and Nedergaard, 2012; Joe et al., 2010; Kajimura et al., 2008; Schulz et al., 2011; Seale et al., 2008; Seale et al., 2007) or *in vivo* (Joe et al., 2010; Kajimura et al., 2008; Schulz et al., 2011; Seale et al., 2008; Seale et al., 2007). In this study, we report that

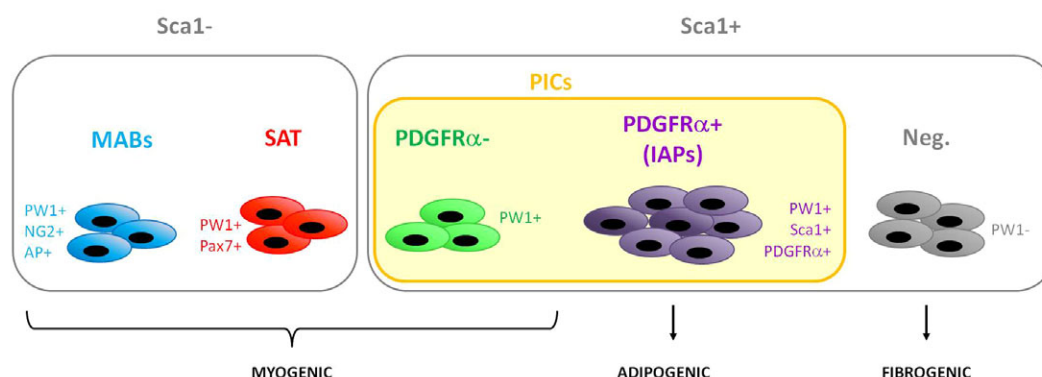


Fig. 7. PW1 expression defines all resident progenitor populations in skeletal muscle. Model representing stem cell hierarchy based on PW1 expression, in which each progenitor population expresses PW1 and at least another specific marker. Myogenic potential resides in satellite cells (SAT), mesoangioblasts (MABs) and a subpopulation of PICs, whereas adipogenic potential arises from the IAP fraction of PICs. Cells that do not express PW1 give rise to fibroblasts. IAPs, interstitial adipogenic progenitors; Neg., PW1⁻/PDGFR α ⁻ cells.

PDGFR α + PICs express brown fat-specific markers (*Ucp1* and *Prdm16*) as well as markers for white/‘beige’ fat (i.e. *Hoxc9*) (Waldén et al., 2012; Wu et al., 2012), suggesting that PDGFR α + PICs can generate ‘beige’ fat cells or a mixture of brown and white/‘beige’ adipocytes. We conclude that PW1 expression identifies at least three progenitor populations in adult muscle: PW1+/PAX7+ (satellite cells), PW1+/PDGFR α + (adipocytes) and myogenic interstitial cells that do not express PAX7 or PDGFR α (Fig. 7). Markers that specifically identify the myogenic fraction of PICs remain to be elucidated. Whether this interstitial myogenic population can be recruited in settings of muscle injury or disease is of interest. When cultured in adipogenic conditions, the myogenic PDGFR α – PICs express genes consistent with adipogenic activation although they fail to generate adipocytes. This raises the possibility that these cells possess the capacity to enter the adipogenic program but require additional signals. SCA1 is a marker widely used to enrich stem cells (Asakura et al., 2002; Benchaoui et al., 2004; Gumley et al., 1995; Tamaki et al., 2002), and is implicated in lineage commitment and stem cell self-renewal (Bonyadi et al., 2003; Ito et al., 2003). Although all interstitial cells with myogenic or adipogenic potential express SCA1 and PW1, we note that SCA1+ cells that do not express PW1 are limited to a fibroblast-like phenotype in the conditions used in this study.

Our analyses of early postnatal skeletal muscle progenitors revealed a transient population of PICs that expresses intermediate levels of SCA1 (SCA1_{MED}), which disappears between 3 and 5 weeks of age. A number of studies have suggested that addition of nuclei to myofibers is a primary mechanism of muscle growth up to 3 weeks of age whereas myofiber volume expansion underlies muscle growth at later stages (White et al., 2010). This switch in the cellular program underlying postnatal muscle growth is also concomitant with a change in the genetic requirement for *Pax7* and *Pax3*. Specifically, loss of *Pax7* and/or *Pax3* prior to 3 weeks of age leads to stunted postnatal growth and poor regeneration whereas loss of *Pax3* and *Pax7* after 3 weeks of age has little effect (Lepper et al., 2009). Taken together, we propose that the transient juvenile population of PICs plays a role during early postnatal muscle growth, either through fusion with myofibers or by providing cues for myogenic progenitors. Whether SCA1_{MED} juvenile PICs fuse with myofibers or progressively upregulate SCA1 expression by 3 weeks of age remains to be investigated. In addition to a difference in levels of SCA1 expression, we note that adult PICs and juvenile SCA1_{MED} and SCA1_{HIGH} PICs express PDGFR α whereas only adult and juvenile SCA1_{HIGH} PICs express TIE2, suggesting that the SCA1_{HIGH} PICs in the juvenile and adult are the same cell population. In addition, we note that the SCA1_{MED} PDGFR α + juvenile population shows weak adipogenic capacity when grown alone compared with the unsorted population, whereas the PDGFR α – population is the only fraction with myogenic potential. This suggests that the cross-talk between myogenic and adipogenic progenitors described in adult muscle by others (Joe et al., 2010; Uezumi et al., 2010) is already present in juvenile in the PIC population.

Our data raise a more fundamental issue with regard to postnatal and adult stem cells. Satellite cells are quiescent and reside in a discrete anatomical location under the myofiber basal lamina, whereas PICs reside in an interstitial location. Nonetheless, these cells are all progenitors that communicate with each other to support tissue integrity and regenerative responses (Pannérec et al., 2012). The observation that all these progenitors express PW1 suggests a common regulatory program. A recent report has shown that PW1 is one member of a group of ten parentally imprinted genes that are

expressed in several somatic stem cell lineages in both mice and humans (Berg et al., 2011; Pannérec et al., 2012). We note that PW1 participates in both intrinsic (p53) and extrinsic (inflammatory cytokine signaling) cell stress responses (Relaix et al., 2000; Relaix et al., 1998; Schwarzkopf et al., 2006), which might reflect a shared response mechanism to cell stress in stem cells. Future work will determine whether this common cell stress response mechanism in stem cells plays a role in pathological outcomes, such as ectopic fat deposition and fibrosis, that are commonly associated with late-stage muscle diseases.

Acknowledgements

We thank C. Blanc and B. Hoareau (Flow Cytometry Core CyPS, Pierre and Marie Curie University, Pitie-Salpetriere Hospital, Paris, France) for their assistance; F. Relaix and S. Alonso-Martin for providing some of the PCR primers for myogenic genes.

Funding

This work was supported by the French Ministry of Research ‘Chaire d’Excellence’ and the Muscular Dystrophy Association of America [D.S.] and the European Community Seventh Framework Program projects OPTISTEM (Optimization of stem cell therapy for degenerative epithelial and muscle diseases contract number Health-F5-2009-223098) and ENDOSTEM (Activation of vasculature associated stem cells and muscle stem cells for the repair and maintenance of muscle tissue-agreement number 241440). The Myology Group is a beneficiary of a Strategic Plan Support from the Association Française contre les Myopathies (AFM) and is affiliated with the Institute of Myology as well the ANR ‘Laboratoire d’Excellence’ program REVIVE and the IHU-ICAN projects. A.P. was supported by the French Ministry of Research and the Fondation pour la Recherche Médicale (Programme ‘Espoirs de la Recherche’, number FDT20110922527).

Competing interests statement

The authors declare no competing financial interests.

Author contributions

All experiments were carried out by A.P. and L.F. using mouse models and reagents generated by V.B. Experimental design, analyses and preparation of the manuscript were carried out by A.P., L.F., V.B., G.M. and D.A.S.

Supplementary material

Supplementary material available online at <http://dev.biologists.org/lookup/suppl/doi:10.1242/dev.089326/-/DC1>

References

- Asakura, A., Seale, P., Girgis-Gabardo, A. and Rudnicki, M. A. (2002). Myogenic specification of side population cells in skeletal muscle. *J. Cell Biol.* **159**, 123–134.
- Benchaoui, R., Rameau, P., Decraene, C., Dreyfus, P., Israeli, D., Piétu, G., Danos, O. and Garcia, L. (2004). Evidence for a resident subset of cells with SP phenotype in the C2C12 myogenic line: a tool to explore muscle stem cell biology. *Exp. Cell Res.* **294**, 254–268.
- Benchaoui, R., Meregalli, M., Farini, A., D’Antona, G., Belicchi, M., Goyenvalle, A., Battistelli, M., Bresolin, N., Bottinelli, R., Garcia, L. et al. (2007). Restoration of human dystrophin following transplantation of exon-skipping-engineered DMD patient stem cells into dystrophic mice. *Cell Stem Cell* **1**, 646–657.
- Berg, J. S., Lin, K. K., Sonnet, C., Boles, N. C., Weksberg, D. C., Nguyen, H., Holt, L. J., Rickwood, D., Daly, R. J. and Goodell, M. A. (2011). Imprinted genes that regulate early mammalian growth are coexpressed in somatic stem cells. *PLoS ONE* **6**, e26410.
- Besson, V., Smeriglio, P., Wegener, A., Relaix, F., Nait Oumesmar, B., Sassoon, D. A. and Marazzi, G. (2011). PW1 gene/paternally expressed gene 3 (PW1/Peg3) identifies multiple adult stem and progenitor cell populations. *Proc. Natl. Acad. Sci. USA* **108**, 11470–11475.
- Bischoff, R. (1975). Regeneration of single skeletal muscle fibers in vitro. *Anat. Rec.* **182**, 215–235.
- Bonyadi, M., Waldman, S. D., Liu, D., Aubin, J. E., Grynepas, M. D. and Stanford, W. L. (2003). Mesenchymal progenitor self-renewal deficiency leads to age-dependent osteoporosis in Sca-1/Ly-6A null mice. *Proc. Natl. Acad. Sci. USA* **100**, 5840–5845.
- Brunelli, S., Tagliafico, E., De Angelis, F. G., Tonlorenzi, R., Baesso, S., Ferrari, S., Niinobe, M., Yoshikawa, K., Schwartz, R. J., Bozzoni, I. et al. (2004). Msx2 and neocdin combined activities are required for smooth muscle differentiation in mesoangioblast stem cells. *Circ. Res.* **94**, 1571–1578.

- Cannon, B. and Nedergaard, J. (2012). Cell biology: neither brown nor white. *Nature* **488**, 286-287.
- Coletti, D., Yang, E., Marazzi, G. and Sassoon, D. (2002). TNF α inhibits skeletal myogenesis through a PW1-dependent pathway by recruitment of caspase pathways. *EMBO J.* **21**, 631-642.
- Dellavalle, A., Sampaoli, M., Tonlorenzi, R., Tagliafico, E., Sacchetti, B., Perani, L., Innocenzi, A., Galvez, B. G., Messina, G., Morosetti, R. et al. (2007). Pericytes of human skeletal muscle are myogenic precursors distinct from satellite cells. *Nat. Cell Biol.* **9**, 255-267.
- Dellavalle, A., Maroli, G., Covarello, D., Azzoni, E., Innocenzi, A., Perani, L., Antonini, S., Sambasivan, R., Brunelli, S., Tajbakhsh, S. et al. (2011). Pericytes resident in postnatal skeletal muscle differentiate into muscle fibres and generate satellite cells. *Nat. Commun.* **2**, 499.
- Fukada, S., Uezumi, A., Ikemoto, M., Masuda, S., Segawa, M., Tanimura, N., Yamamoto, H., Miyagoe-Suzuki, Y. and Takeda, S. (2007). Molecular signature of quiescent satellite cells in adult skeletal muscle. *Stem Cells* **25**, 2448-2459.
- Gross, J. G. and Morgan, J. E. (1999). Muscle precursor cells injected into irradiated mdx mouse muscle persist after serial injury. *Muscle Nerve* **22**, 174-185.
- Gumley, T. P., McKenzie, I. F. and Sandrin, M. S. (1995). Tissue expression, structure and function of the murine Ly-6 family of molecules. *Immunol. Cell Biol.* **73**, 277-296.
- Gussoni, E., Soneoka, Y., Strickland, C. D., Buzney, E. A., Khan, M. K., Flint, A. F., Kunkel, L. M. and Mulligan, R. C. (1999). Dystrophin expression in the mdx mouse restored by stem cell transplantation. *Nature* **401**, 390-394.
- Ito, C. Y., Li, C. Y., Bernstein, A., Dick, J. E. and Stanford, W. L. (2003). Hematopoietic stem cell and progenitor defects in Sca-1/Ly-6A-null mice. *Blood* **101**, 517-523.
- Joe, A. W., Yi, L., Natarajan, A., Le Grand, F., So, L., Wang, J., Rudnicki, M. A. and Rossi, F. M. (2010). Muscle injury activates resident fibro/adipogenic progenitors that facilitate myogenesis. *Nat. Cell Biol.* **12**, 153-163.
- Kajimura, S., Seale, P., Tomaru, T., Erdjument-Bromage, H., Cooper, M. P., Ruas, J. L., Chin, S., Tempst, P., Lazar, M. A. and Spiegelman, B. M. (2008). Regulation of the brown and white fat gene programs through a PRDM16/CtBP transcriptional complex. *Genes Dev.* **22**, 1397-1409.
- Konigsberg, I. R. (1961). Cellular differentiation in colonies derived from single cells platings of freshly isolated chick embryo muscle cells. *Proc. Natl. Acad. Sci. USA* **47**, 1868-1872.
- Lee, Y. H., Petkova, A. P., Mottillo, E. P. and Granneman, J. G. (2012). In vivo identification of bipotential adipocyte progenitors recruited by β 3-adrenoceptor activation and high-fat feeding. *Cell Metab.* **15**, 480-491.
- Lepper, C., Conway, S. J. and Fan, C. M. (2009). Adult satellite cells and embryonic muscle progenitors have distinct genetic requirements. *Nature* **460**, 627-631.
- Liadaki, K., Casar, J. C., Wessen, M., Luth, E. S., Jun, S., Gussoni, E. and Kunkel, L. M. (2012). β 4 integrin marks interstitial myogenic progenitor cells in adult murine skeletal muscle. *J. Histochem. Cytochem.* **60**, 31-44.
- Mauro, A. (1961). Satellite cell of skeletal muscle fibers. *J. Biophys. Biochem. Cytol.* **9**, 493-495.
- Messina, G., Sirabella, D., Monteverde, S., Galvez, B. G., Tonlorenzi, R., Schnapp, E., De Angelis, L., Brunelli, S., Relaix, F., Buckingham, M. et al. (2009). Skeletal muscle differentiation of embryonic mesoangioblasts requires pax3 activity. *Stem Cells* **27**, 157-164.
- Mitchell, K. J., Pannérec, A., Cadot, B., Parlakian, A., Besson, V., Gomes, E. R., Marazzi, G. and Sassoon, D. A. (2010). Identification and characterization of a non-satellite cell muscle resident progenitor during postnatal development. *Nat. Cell Biol.* **12**, 257-266.
- Montarras, D., Morgan, J., Collins, C., Relaix, F., Zaffran, S., Cumano, A., Partridge, T. and Buckingham, M. (2005). Direct isolation of satellite cells for skeletal muscle regeneration. *Science* **309**, 2064-2067.
- Murphy, M. M., Lawson, J. A., Mathew, S. J., Hutcheson, D. A. and Kardon, G. (2011). Satellite cells, connective tissue fibroblasts and their interactions are crucial for muscle regeneration. *Development* **138**, 3625-3637.
- Natarajan, A., Lemos, D. R. and Rossi, F. M. (2010). Fibro/adipogenic progenitors: a double-edged sword in skeletal muscle regeneration. *Cell Cycle* **9**, 2045-2046.
- Pallafacchina, G., François, S., Regnault, B., Czarny, B., Dive, V., Cumano, A., Montarras, D. and Buckingham, M. (2010). An adult tissue-specific stem cell in its niche: a gene profiling analysis of in vivo quiescent and activated muscle satellite cells. *Stem Cell Res.* **4**, 77-91.
- Pannérec, A., Marazzi, G. and Sassoon, D. (2012). Stem cells in the hood: the skeletal muscle niche. *Trends Mol. Med.* **18**, 599-606.
- Pessina, P., Conti, V., Tonlorenzi, R., Touvier, T., Meneveri, R., Cossu, G. and Brunelli, S. (2012). Necdin enhances muscle reconstitution of dystrophic muscle by vessel-associated progenitors, by promoting cell survival and myogenic differentiation. *Cell Death Differ.* **19**, 827-838.
- Relaix, F., Weng, X., Marazzi, G., Yang, E., Copeland, N., Jenkins, N., Spence, S. E. and Sassoon, D. (1996). Pw1, a novel zinc finger gene implicated in the myogenic and neuronal lineages. *Dev. Biol.* **177**, 383-396.
- Relaix, F., Wei, X. J., Wu, X. and Sassoon, D. A. (1998). Peg3/Pw1 is an imprinted gene involved in the TNF-NF κ B signal transduction pathway. *Nat. Genet.* **18**, 287-291.
- Relaix, F., Wei, X., Li, W., Pan, J., Lin, Y., Bowtell, D. D., Sassoon, D. A. and Wu, X. (2000). Pw1/Peg3 is a potential cell death mediator and cooperates with Siah1a in p53-mediated apoptosis. *Proc. Natl. Acad. Sci. USA* **97**, 2105-2110.
- Relaix, F., Rocancourt, D., Mansouri, A. and Buckingham, M. (2005). A Pax3/Pax7-dependent population of skeletal muscle progenitor cells. *Nature* **435**, 948-953.
- Sampaoli, M., Torrente, Y., Innocenzi, A., Tonlorenzi, R., D'Antona, G., Pellegrino, M. A., Barresi, R., Bresolin, N., De Angelis, M. G., Campbell, K. P. et al. (2003). Cell therapy of alpha-sarcoglycan null dystrophic mice through intra-arterial delivery of mesoangioblasts. *Science* **301**, 487-492.
- Sampaoli, M., Blot, S., D'Antona, G., Granger, N., Tonlorenzi, R., Innocenzi, A., Mogno, P., Thibaud, J. L., Galvez, B. G., Barthélémy, I. et al. (2006). Mesoangioblast stem cells ameliorate muscle function in dystrophic dogs. *Nature* **444**, 574-579.
- Schulz, T. J., Huang, T. L., Tran, T. T., Zhang, H., Townsend, K. L., Shadrach, J. L., Cerletti, M., McDougall, L. E., Giorgadze, N., Tchkonja, T. et al. (2011). Identification of inducible brown adipocyte progenitors residing in skeletal muscle and white fat. *Proc. Natl. Acad. Sci. USA* **108**, 143-148.
- Schwarzkopf, M., Coletti, D., Sassoon, D. and Marazzi, G. (2006). Muscle cachexia is regulated by a p53-PW1/Peg3-dependent pathway. *Genes Dev.* **20**, 3440-3452.
- Seale, P., Kajimura, S., Yang, W., Chin, S., Rohas, L. M., Uldry, M., Tavernier, G., Langin, D. and Spiegelman, B. M. (2007). Transcriptional control of brown fat determination by PRDM16. *Cell Metab.* **6**, 38-54.
- Seale, P., Bjork, B., Yang, W., Kajimura, S., Chin, S., Kuang, S., Scimè, A., Devarakonda, S., Conroe, H. M., Erdjument-Bromage, H. et al. (2008). PRDM16 controls a brown fat/skeletal muscle switch. *Nature* **454**, 961-967.
- Tamaki, T., Akatsuka, A., Ando, K., Nakamura, Y., Matsuzawa, H., Hotta, T., Roy, R. R. and Edgerton, V. R. (2002). Identification of myogenic-endothelial progenitor cells in the interstitial spaces of skeletal muscle. *J. Cell Biol.* **157**, 571-577.
- Uezumi, A., Fukada, S., Yamamoto, N., Takeda, S. and Tsuchida, K. (2010). Mesenchymal progenitors distinct from satellite cells contribute to ectopic fat cell formation in skeletal muscle. *Nat. Cell Biol.* **12**, 143-152.
- Uezumi, A., Ito, T., Morikawa, D., Shimizu, N., Yoneda, T., Segawa, M., Yamaguchi, M., Ogawa, R., Matev, M. M., Miyagoe-Suzuki, Y. et al. (2011). Fibrosis and adipogenesis originate from a common mesenchymal progenitor in skeletal muscle. *J. Cell Sci.* **124**, 3654-3664.
- Waldén, T. B., Hansen, I. R., Timmons, J. A., Cannon, B. and Nedergaard, J. (2012). Recruited vs. nonrecruited molecular signatures of brown, "brite," and white adipose tissues. *Am. J. Physiol.* **302**, E19-E31.
- White, R. B., Biérinx, A. S., Gnocchi, V. F. and Zammit, P. S. (2010). Dynamics of muscle fibre growth during postnatal mouse development. *BMC Dev. Biol.* **10**, 21.
- Wu, J., Boström, P., Sparks, L. M., Ye, L., Choi, J. H., Giang, A. H., Khandekar, M., Virtanen, K. A., Nuutila, P., Schaart, G. et al. (2012). Beige adipocytes are a distinct type of thermogenic fat cell in mouse and human. *Cell* **150**, 366-376.
- Zammit, P. S., Relaix, F., Nagata, Y., Ruiz, A. P., Collins, C. A., Partridge, T. A. and Beauchamp, J. R. (2006). Pax7 and myogenic progression in skeletal muscle satellite cells. *J. Cell Sci.* **119**, 1824-1832.